

INTERACTION OF SUPERNOVA REMNANTS WITH INTERSTELLAR CLOUDS: FROM THE NOVA LASER TO THE GALAXY

RICHARD I. KLEIN

Department of Astronomy, University of California, Berkeley, 601 Campbell Hall, Berkeley, CA 94270; and Lawrence Livermore National Laboratory, P.O. Box 808, Livermore, CA 94550

AND

KIMBERLY S. BUDIL, THEODORE S. PERRY, AND DAVID R. BACH

Lawrence Livermore National Laboratory, P.O. Box 808, Livermore, CA 94550

Received 1999 January 19; accepted 1999 October 8

ABSTRACT

The interaction of strong shock waves, such as those generated by the explosion of supernovae with interstellar clouds, is a problem of fundamental importance in understanding the evolution and the dynamics of the interstellar medium (ISM) as it is disrupted by shock waves. The physics of this essential interaction sheds light on several key questions: (1) What is the rate and total amount of gas stripped from the cloud, and what are the mechanisms responsible? (2) What is the rate of momentum transfer to the cloud? (3) What is the appearance of the shocked cloud, its morphology and velocity dispersion? (4) What is the role of vortex dynamics on the evolution of the cloud? (5) Can the interaction result in the formation of a new generation of stars? To address these questions, one of us has embarked on a comprehensive multidimensional numerical study of the shock cloud problem using high-resolution adaptive mesh refinement (AMR) hydrodynamics. Here we present the results of a series of Nova laser experiments investigating the evolution of a high-density sphere embedded in a low-density medium after the passage of a strong shock wave, thereby emulating the supernova shock-cloud interaction. The Nova laser was utilized to generate a strong (\sim Mach 10) shock wave which traveled along a miniature beryllium shock tube, 750 μm in diameter, filled with a low-density plastic emulating the ISM. Embedded in the plastic was a copper microsphere (100 μm in diameter) emulating the interstellar cloud. Its morphology and evolution as well as the shock wave trajectory were diagnosed via side-on radiography. We describe here experimental results of this interaction for the first time out to several cloud crushing times and compare them to detailed two- and three-dimensional radiation hydrodynamic simulations using both arbitrary Lagrangian and Eulerian hydrodynamics (ALE) as well as high-resolution AMR hydrodynamics. We briefly discuss the key hydrodynamic instabilities instrumental in destroying the cloud and show the importance of inherently three-dimensional instabilities and their role in cloud evolution. We describe the relationship of these new experiments and calculations to recent *ROSAT* X-ray observations in the Cygnus Loop.

Subject headings: hydrodynamics — ISM: general — shock waves — supernova remnants

1. INTRODUCTION

The interaction of shock waves in the interstellar medium (ISM), such as those associated with supernovae, stellar winds, bipolar flows, H II regions, or spiral density waves with interstellar clouds is a fundamental problem in interstellar gas dynamics and is crucial to understanding the evolution of the ISM. The physics of this essential interaction sheds light on several key questions: (1) What is the rate and total amount of gas stripped from the cloud, and what are the mechanisms responsible? (2) What is the rate of momentum transfer to the cloud? (3) What is the appearance of the shocked cloud, its morphology and velocity dispersion? (4) What is the role of vortex dynamics on the evolution of the cloud? (5) Can the interaction result in the formation of a new generation of stars? The investigation of this highly nonlinear interaction is not amenable to analytic approaches and requires a detailed multidimensional hydrodynamic study of the cloud shock problem using high-resolution numerical methods. Such an approach has been made by Klein, McKee, & Colella (1994), who found that the cloud can be destroyed by a series of instabilities associated with the postshock flow of intercloud gas past the

cloud. Earlier work on this important problem includes that of Woodward (1976) and Nittman, Falle, & Gaskell (1982). More recent work that investigates the deposition of vorticity associated with the shock bubble interaction and the evolution of vortex structures can be found in Zabusky et al. (1998) and Ray & Zabusky (2000). Recently, Levenson et al. (1997) have performed a detailed X-ray survey of the Cygnus Loop supernova remnant with the *ROSAT* high-resolution imager (HRI). The Cygnus Loop is the prototype for a supernova remnant (SNR) that is dominated by ISM-shock interactions. The Cygnus Loop provides key observations showing the basic inhomogeneity of the ISM and the fundamental nature of cloud shock interactions and their role in determining the X-ray morphology of the supernova remnant. In this paper, we describe a set of new experiments performed for the first time on the Nova laser to investigate this fundamental fluid dynamical interaction and to shed light on recent astronomical observations. Detailed multidimensional hydrodynamic simulations have been compared with the experiments and are briefly described. For a more detailed discussion of these experiments, the associated calculations and comparisons with

observations the reader is referred to Klein et al. (2000).

2. EXPERIMENTAL SETUP

Strong shock waves produced in a radiation-driven CH target by laser produced X-rays were driven through a copper sphere. The motion and growth of the interaction were measured using shadowgrams produced by a large area X-ray backlighter produced by laser light. The sphere became hydrodynamically distorted after the passage of the shock, having a complicated downstream structure. This was an instability-induced structure which was predicted by calculations. The experiment is a convenient laboratory analog of the interactions occurring between supernova driven shocks and interstellar clouds. In addition, the experiment is important for providing validation data for three-dimensional codes.

A schematic description of the experiment is shown in Figure 1. The diagram is not to scale, and the area of the target package is greatly expanded. Eight Nova laser beams were focused into a cylindrical gold hohlraum (Lindl 1995) producing a broad spectrum of X-rays which ablated the surface of the brominated plastic. The bromine dopant was included in the plastic to prevent preheat from high-energy X-rays produced in the hohlraum. The relatively planar shock wave produced by the ablation traveled down the cylinder, passing the copper sphere. Two additional laser beams impinged on a backlight target (titanium) and produced line radiation at about 4.5 keV, which passed through the cylinder perpendicular to its axis and were detected by the imaging camera. Differences in optical density to the backlight X-rays formed a shadowgram

which allowed positional information on the shock front and the sphere to be obtained.

Titanium was chosen as the backlight because its characteristic radiation at 4.5 keV is completely stopped by even small amounts of copper, which allows accurate imaging of the breakup of the copper spheres. Also, there is a clear difference in absorption at this photon energy between the shocked and unshocked plastic. Eight of the 10 Nova laser beams were used to heat the hohlraum, and the two remaining beams were defocused on the backlight target to produce a radiation source which was oval shaped with a diameter of 800 μm . Since the objective was to measure the positions of both the shock front and the sphere as a function of time, the delays of the backlight beams were varied from 20 to 70 ns after the beginning of the laser pulse. The camera was opened 0.5 ns after the start of the backlight beams. The heating laser pulse width was 1.0 ns in length, and the backlight pulse widths were 3.0 ns. Using a standard Nova diagnostic, the flexible X-ray imager (Budil et al. 1996), four time snapshots could be taken during the backlighter pulse. It was necessary to make a correction for parallax to the positions measured on the film, as there were significantly varying angles between the axis of the camera and the line between the strips and the target. The data were extracted from the film after digitizing and analyzing the digitized data using a two-dimensional image analysis program (D. W. Phillion 1996, private communication).

3. RESULTS

Figure 2 shows a series of sphere-shock shadowgrams obtained from times from 20 to 26.5 ns after the laser pulse and show the early time crushing of the sphere. In this

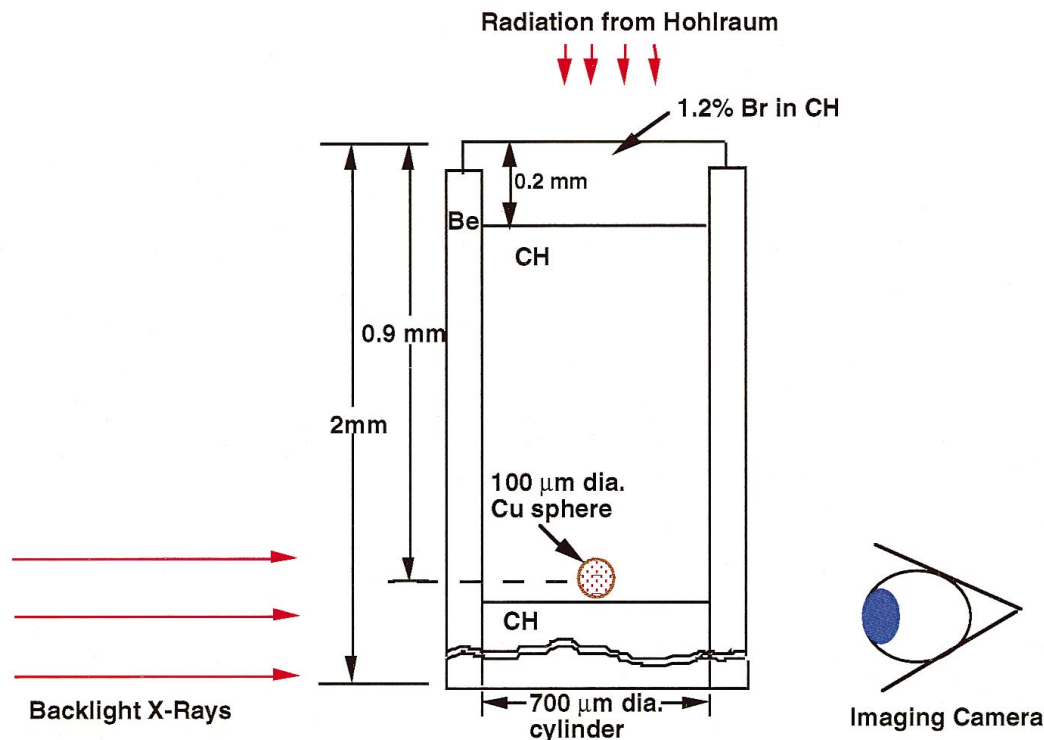


FIG. 1.—Schematic arrangement of experiment (not to scale) showing a cross section through a cylindrical target used for the sphere experiment. The dimensions given on the package are nominal and were varied from experiment to experiment.

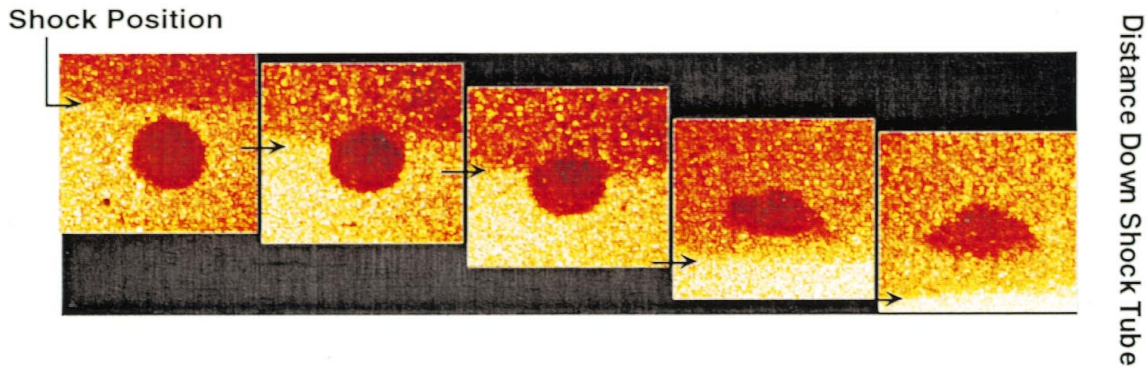


FIG. 2.—Sphere-shock shadowgrams. These were obtained at times from 20 to 26.5 ns after the laser pulse and show the early time crushing of the sphere.

series, we clearly note the propagation of the Mach 10 shock through the sphere. The sphere undergoes significant compression and shows the initial behavior of Kelvin-Helmholtz instabilities around the sides of the sphere due to shear flow between the sphere and the surrounding plastic, induced by shock diffraction around the sides.

Figure 3 shows the sphere at a later time in its evolution in the first panel, together with two-dimensional (*middle panel*) and three-dimensional calculations (*third panel*) of the shock-sphere interaction. The comparisons are made at 3.0 crushing times where a crushing time t_{cc} (Klein et al. 1994) is defined as the time required for the shock to traverse the sphere and is given by

$$t_{cc} = (\rho_{cl}/\rho_{ISM})^{1/2}(a_{cl}/v_{shock}),$$

where ρ_{cl} is the cloud density, ρ_{ISM} is the density of the ISM or in the experiment the density of the surrounding foam,

a_{cl} is the sphere radius, and v_{shock} is the shock velocity in the interstellar medium or in the experiment, the velocity in the foam. The crushing time in this experiment was about 8 ns. This time represents a stage in the shock sphere evolution where the sphere is crushed on both sides due to shock induced pressures.

Two-dimensional CALE is an arbitrary Lagrange-Eulerian multifluid hydrodynamic code using realistic equation of state data (cf. Kane et al. 1997). Three-dimensional AMR is a single fluid adaptive mesh refinement calculation assuming an ideal gas equation of state (ESO) (cf. Klein et al. 1994). In Figure 3, the shock wave has originated from the top and has traversed the sphere by moving downward. The experimental data (*left*) shows that at $3.0t_{cc}$ the sphere has undergone a severe instability and shows a significant separation between the front (*top*) and the back (*bottom*). This separation results in a voiding in the

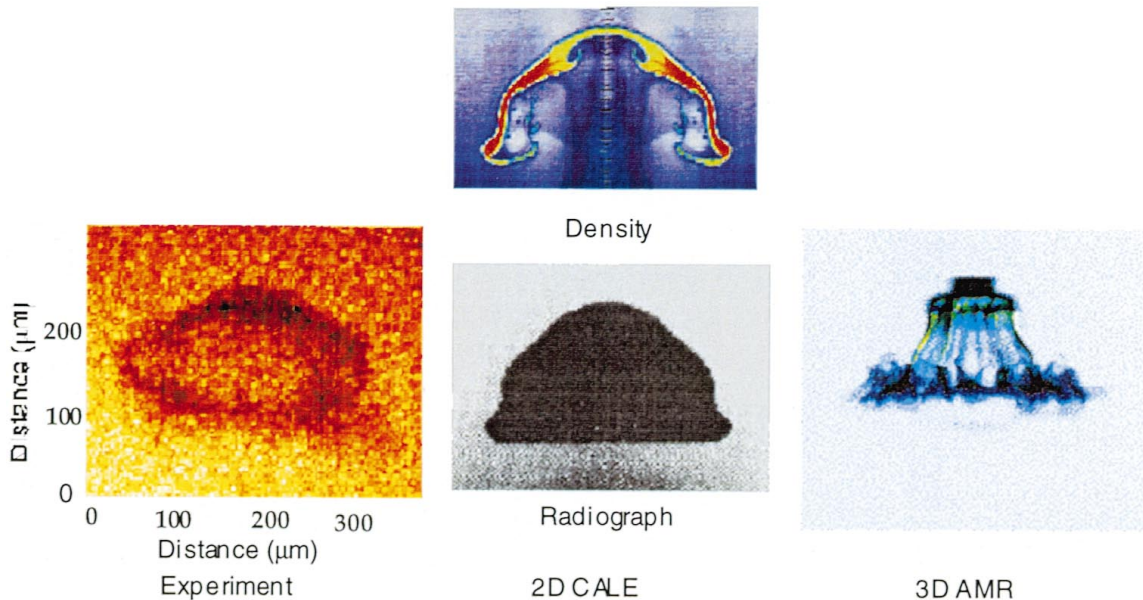


FIG. 3.—A comparison of the experimental radiograph of the sphere (*left*) taken at three crushing times with two-dimensional (*middle*), and three-dimensional (*right*) AMR calculations. The middle panel shows the two-dimensional CALE theoretical radiograph (*bottom*) and a two-dimensional isodensity image (*top*) on the same spatial scale as the experimental radiograph. The bifurcation in the sphere seen in the experiment occurs only with the three-dimensional calculation. The three-dimensional AMR calculations with ideal EOS are scale-free and are meant to show the breakup of the sphere due to vortex ring instabilities.

sphere. The two-dimensional CALE calculation (*middle*) shows a simulated radiograph at this time. The two-dimensional calculation does a good job in getting the overall morphology of the sphere correct, but indicates no such separation of the front and back of the sphere. The two-dimensional calculations had a resolution of 50 cells per initial sphere radius (R_{50}) in a region surrounding the sphere that is 2.5 sphere radii in the radial direction and 6 sphere radii in the axial direction; thus the sphere traversed a region that was 125 cells by 300 cells throughout its evolution. This resolution (R_{50}) was found to be reasonably converged through a detailed convergence study of several global quantities (Klein et al. 1994). The entire experimental domain (cf. Fig. 1, $700 \mu\text{m} \times 2000 \mu\text{m}$) is included in the computational domain. The resolution outside of the region that encompasses the sphere is 25 cells per initial cloud radius. Although this resolution is degraded from the resolution surrounding the sphere, it is the region around the sphere that crucially requires high resolution. The three-dimensional AMR simulation (*right*), on the other hand, shows that the sphere undergoes severe nonaxisymmetric instabilities resulting in a fluted structure in the lower half. This structure is well resolved. The three-dimensional AMR simulations had a resolution of R_{90} (90 cells per initial sphere radius). The lower part of the sphere has a diameter of five initial sphere radii, thus the fluted structure was about 450 cells across. The structure is more highly fragmented and considerably less coherent than in two dimensions at a comparable time. As we pointed out, the two-dimensional calculation has a resolution that is reasonably well converged, thus the significant differences in the two- and three-dimensional calculations appear to be due to real physical effects, not diffusivity due to lack of resolution. In three dimensions the sphere undergoes azimuthal bending mode instabilities in a powerful vortex ring that forms in the back part (*bottom*) of the shocked sphere. This is analogous to the Widnall instability in incompressible flow. This results in the breaking up of the strong vortex ring associated with the sphere, into smaller less coherent vortex structures. The three-dimensional results indicate that this breaking up of the vortex ring by a Widnall-like instability results in the voiding in the sphere in reasonable agreement with the experiment. Coherent vortex rings found in two-dimensional simulations are unstable in three dimensions and would result in more effective mixing and turbulence in three dimensions. The transition to turbulence in the evolution of the sphere is discussed in Klein et al. (2000). An elucidation of the dynamical properties of the vortex ring and the role of nonaxisymmetric instabilities in vortex rings causing the bifurcation of the sphere requires careful three-dimensional calculations with realistic equations of state. We are in the process of performing such calculations. The nature of the breakup of the vortex ring await these three-dimensional calculations and the nature of the bending mode instability will be studied in detail. This will be discussed further in a separate paper.

Figure 4 shows the shock and sphere positions as a function of time after the beginning of the heating laser pulse. The shock positions were measured on a vertical line through the center of the sphere. This was done because there was some variation in the shock position in the lateral direction, probably due to nonuniformity in drive. The sphere position was that measured for the center of the spheres, even though in many cases later in time, the sphere

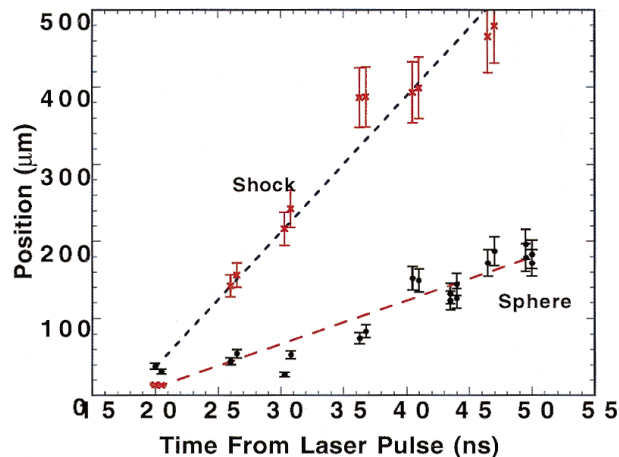


FIG. 4.—Results of the shock-sphere experiment showing the position of the shock front and the position of the center of the sphere as a function of time after the beginning of the heating laser pulse. The zero of the ordinate is the position of the sphere before the beginning of the drive. The shock front was measured in a vertical line passing through the center of the sphere, as the shock fronts were not always parallel to the horizontal axis.

was definitely not spherical. The velocity of the sphere in the background foam is in reasonable agreement with the simple drag theory developed by Klein et al. (1994) and will be discussed separately.

Our experiment is showing the first evidence of three-dimensional bending mode instabilities in shock-sphere interactions at high Mach number. The crucial aspects of this instability can be understood by high-resolution, three-dimensional hydrodynamic calculations, but are not well represented by two-dimensional calculations. Later time evolution of the shock-sphere interaction experiment shows the transition from the breakup of the sphere due to bending mode and Kelvin Helmholtz instabilities to the turbulent regime with structure present on a wide range of scales. These experiments are potentially promising in understanding the interaction of supernova blast waves with interstellar clouds. Klein et al. (1994) demonstrated that the physics of this interaction can be well understood by consideration of the density ratio of the cloud to the intercloud medium and the Mach number of the shock. They show that by consideration of these two parameters, the evolution of a sphere after interaction with a strong shock is scale invariant for the case of nonradiative shocks. They apply their calculations for a Mach 10 shock to the interaction of the supernova remnant in the Cygnus Loop with the Southwestern Cloud. By conducting a series of shock sphere laser experiments examining the sensitivity of the interaction to the variation of these parameters, we hope to be able to scale the experiments to actual structures in the Cygnus Loop. The greatly improved sensitivity and spatial resolution of the *ROSAT* HRI X-ray observations make it ideal for exploring blast wave-cloud interactions. The combination of these high-resolution *ROSAT* observations with our Nova laser experiments and high-resolution three-dimensional AMR calculations gives us a unique approach to studying this fundamental interaction in the ISM.

This work was performed under the auspices of the US Department of Energy by the Lawrence Livermore National Laboratory under Contract W-7405-ENG-48.

REFERENCES

- Budil, K. S., Perry, T. S., Bell, P. M., Hares, J. D., Miller, P. L., Peyser, T. A., Wallace, R., Louis, H., & Smith, D. E. 1996, *Rev. Sci. Instrum.*, *67*, 485
- Kane, J., et al. 1997, *ApJ*, *478*, L75
- Klein, R. I., Budil, K. S., Perry, T. S., & Bach, D. R. 2000, in preparation
- Klein, R. I., McKee, C. F., & Colella, P. 1994, *ApJ*, *420*, 213
- Levenson, N. A., et al. 1997, *ApJ*, *484*, 304
- Lindl, J. 1995, *Phys. Plasmas*, *2* (11), 3933
- Nittman, J., Falle, S., & Gaskell, P. H. 1982, *MNRAS*, *201*, 833
- Ray, J., & Zabusky, N. 2000, *ApJS*, submitted
- Woodward, P. R. 1976, *ApJ*, *207*, 484
- Zabusky, N. J., & Zeng, S. M. 1998, *J. Fluid Mech.*, *362*, 327